Preprints of the 21st IFAC World Congress (Virtual)
Berlin, Germany, July 12-17, 2020

Online Inertial Parameter Estimation for Robotic Loaders ⋆

Martín Calvo Sánchez * **Miguel Torres-Torriti** *
Fernando Auat Cheein **

* *Department of Electrical Engineering, Pontificia Universidad Católica de Chile, Av. Vicuña Mackenna 4860, Macul, Santiago, Chile (e-mail: mdcalvo@uc.cl; mtorrest@ing.puc.cl).*
** *Department of Electronic Engineering, Universidad Técnica Federico Santa María, Av. España 1680, Valparaiso, Chile (e-mail: fernando.auat@usm.cl).*

Abstract: Payload estimation is essential to measure productivity, evaluate efficiency in industrial operations and adapting control laws according to the carried weight. One particular problem is to identify how much mass is carried in a mining machine while it is being operated without using strain gauge sensors which require frequent calibration and are prone to failure due to mechanical stress. This paper presents an on-line method to estimate a loader's payload mass, rotational inertia and viscous friction coefficients employing inertial, torque and speed measurements. The proposed approach introduces a mutual information criterion to select those acceleration and velocity measurements that jointly with the excitation force ensure the identifiability of the parameters. The approach relies on the recursive least-squares algorithm for fast update of the parameters. The proposed strategy is also compared to the implementations based on variants of the least-squares estimator, such as the feasible generalized least squares and the total least squares approach. The approach is tested in simulation and validated in experiments with an industrial semi-autonomous skid-steer loader Cat®262C for different loads. Results show that using the recursive least squares it is possible to estimate the parameters with the same level of accuracy than OLS approach, while not needing a large buffer for estimation. Mass is effectively estimated with an RMS error below 1% the total mass of the machine.

Keywords: Mobile robots, inertial parameters, on-line recursive parameter estimation, identification methods, autonomous vehicles.

1. INTRODUCTION

Improving excavation and hauling efficiency is crucial to mining productivity. In recent years significant efforts have been devoted to the implementation of teleoperation capabilities and autonomous machines (Rigotti-Thompson et al., 2018; Aguilera-Marinovic et al., 2017). However, a central aspect in productivity and efficiency concerns the amount of material extracted at the draw point and the associated energy consumption. Thus measuring productivity requires information of the inertial parameters, particularly the transported mass.

One way to measure the load of an excavator or a load-haul-dump (LHD) vehicle is to employ strain gauge sensors. Unfortunately, these sensors are susceptible to quick degradation due to continuous deformations and thus demand frequent recalibration that renders these sensors unreliable and not very practical in the context of mining operations. An alternative approach is to estimate the load by model identification methods using information from other sensors. In this work we propose a strategy that relies on inertial, torque and velocity sensors to estimate the inertial parameters of loaders, e.g. scoops, LHD vehicles, dump trucks, skid-steer loaders. The proposed approach combines classic least squares estimators, but includes strategies that provide information quality metrics essential to ensuring that the inertial parameter estimates can be computed online in real-time without degrading the accuracy of the estimates, particularly at constant speed or low torque conditions for which the estimation problem becomes ill-conditioned.

Methods for estimating inertial parameters and mobile robot model identification have been proposed in (Hoang and Kang, 2015; Rogers-Marcovitz and Kelly, 2014; Seegmiller et al., 2013). However, none of the existing approaches have focused on the particular challenges of inertial parameter estimation of robotic excavators and loaders for mining. Most of the approaches are validated only in simulation (Hoang and Kang, 2015) or consider other applications, such as the inertial load modeling of an object grasped by several mobile manipulator robots (Franchi et al., 2014) or estimating wheel-terrain slippage characteristics (Rogers-Marcovitz and Kelly, 2014). Most of the existing inertial parameter estimation approaches either consider robot arms with fixed-bases or constant mass

⋆ This project has been supported by the National Commission for Science and Technology Research of Chile (Conicyt) under Fondecyt grant 1171760, Basal FB0008 and Fondequip grant 120141.

mobile robots. The majority focus on the identification of the end-effector load (Kubus et al., 2008; Siciliano and Khatib, 2008) and very few have been conceived for online estimation (Kubus et al., 2008).

The contribution of this work can be summarized in the development of a novel approach for reliably computing the inertial parameters of robotic mobile manipulators in *real-time* and *online*. The approach takes advantage of the structure of the model equations and introduces the use of a mutual information criterion to select measurements that jointly with the excitation force can deliver better estimates for the inertial parameters. The proposed approach employs the recursive-least estimator for computational efficiency, but results using ordinary least squares, feasible generalized least squares, total least squares are also obtained for comparison purposes.

The proposed method is especially valuable to operation managers for production monitoring and yield estimation in mining, forestry, construction and other industries that employ a variety of loaders and excavators. On the other hand, the heavy loads moved by these machines, combined with the slope of the terrain and load position can compromise the stability of the machine. Thus it is important to determine in an automated way the inertial characteristics of the machine without employing the less reliable strain gauge sensors for weight measurement.

This paper is organized as follows. Section 2 describes the relevant model equations for the motion dynamics of mobile robotic loader. Section 3 explains the inertial parameter estimation strategy. Section 4 describes the simulations and experiments used to test the proposed approach and presents the results obtained during tests with an industrial robotic mobile manipulator (Aguilera-Marinovic et al., 2017). Finally, Section 5 discusses the conclusions and aspects concerning ongoing research.

2. THEORETICAL BACKGROUND AND EXISTING APPROACHES

Briefly stated, the problem of estimating the inertial parameters of a rigid body b is to find its 10 inertial parameters: the body mass $m^b \in \mathbb{R}$, the center of mass $\boldsymbol{c}_0^b \in \mathbb{R}^3$ relative to an origin $\mathcal{O}^0$ of an inertial coordinate frame $\mathcal{F}_0$, and the six inertia values of the symmetric inertia matrix $\boldsymbol{I}^b \in \mathbb{R}^{3\times3}$ referred the origin $\mathcal{O}^b$ of the body-frame $\mathcal{F}_b$. The rigid body can be considered to be composed of a mobile base, the arm links, the external load held by the arm or a composition of rigidly fixed bodies treated as a single larger body (Siciliano and Khatib, 2008). The estimation procedure then typically involves the following main steps:

(1) Formulating the Newton-Euler equations of the body dynamics to obtain a linear dependence on the inertial parameters.
(2) Generating an adequate motion trajectory.
(3) Measuring with suitable sensors and filters the body velocity $\boldsymbol{v}^b$ and acceleration $\boldsymbol{a}^b$, and the forces or torques.
(4) Solving a least-squares optimization problem to find the parameters that minimize the residuals between the measured values and the value provided by the model.

Using the spatial vector formalism (Featherstone, 2008), the Newton-Euler equation referred to $\mathcal{O}^b$ for a body b is given by

$$\mathbf{f}^b = \mathbf{I}^b\mathbf{a}^b + \mathbf{v}^b \times^* \mathbf{I}^b\mathbf{v}^b \tag{1}$$

where $\mathbf{f}^b$ is the net spatial force acting on body b, $\mathbf{I}^b$ is the spatial inertia matrix

$$\mathbf{I}^b = \begin{bmatrix} \boldsymbol{I}^b & m^b\boldsymbol{S}(\boldsymbol{c}^b) \\ m^b\boldsymbol{S}(\boldsymbol{c}^b)^T & m^b\mathbf{1} \end{bmatrix}$$

and $\mathbf{a}^b$ is the spatial acceleration vector

$$\mathbf{a}^b = \begin{bmatrix} \dot{\boldsymbol{\omega}}^b \\ \dot{\boldsymbol{v}}^b \end{bmatrix} = \begin{bmatrix} \dot{\boldsymbol{\omega}}^b \\ \ddot{\boldsymbol{d}}_0^b - \boldsymbol{\omega}^b \times \boldsymbol{v}^b \end{bmatrix}$$

with $\boldsymbol{S}(\boldsymbol{v}_1)$ denoting the skew-symmetric 3×3 matrix that satisfies $\boldsymbol{S}(\boldsymbol{v}_1)\boldsymbol{v}_2 = \boldsymbol{v}_1 \times \boldsymbol{v}_2$ for any two vectors $\boldsymbol{v}_1, \boldsymbol{v}_2 \in \mathbb{R}^3$, see ch. 2 of (Siciliano and Khatib, 2008) for further details.

Multiplying the spatial inertia and the spatial acceleration yields the first term of the Newton-Euler equation:

$$\mathbf{I}^b\mathbf{a}^b = \begin{bmatrix} \boldsymbol{I}^b\dot{\boldsymbol{\omega}}^b + m^b\boldsymbol{S}(\boldsymbol{c}^b)\left(\ddot{\boldsymbol{d}}_0^b - \boldsymbol{\omega}^b \times \boldsymbol{v}^b\right) \\ m^b\boldsymbol{S}(\boldsymbol{c}^b)^T\dot{\boldsymbol{\omega}}^b + m^b\left(\ddot{\boldsymbol{d}}_0^b - \boldsymbol{\omega}^b \times \boldsymbol{v}^b\right) \end{bmatrix} \tag{2}$$

Similarly, using the expression for the spatial inertia and the spatial velocity

$$\mathbf{v}^b = \begin{bmatrix} \boldsymbol{\omega}^b \\ \boldsymbol{v}^b \end{bmatrix}$$

yields

$$\begin{aligned} \mathbf{v}^b \times^* \mathbf{I}^b\mathbf{v}^b &= \begin{bmatrix} \boldsymbol{S}(\boldsymbol{\omega}^b) & \boldsymbol{S}(\boldsymbol{v}^b) \\ \mathbf{0} & \boldsymbol{S}(\boldsymbol{\omega}^b) \end{bmatrix} \times \begin{bmatrix} \boldsymbol{I}^b & m^b\boldsymbol{S}(\boldsymbol{c}^b) \\ m^b\boldsymbol{S}(\boldsymbol{c}^b)^T & m^b\mathbf{1} \end{bmatrix} \begin{bmatrix} \boldsymbol{\omega}^b \\ \boldsymbol{v}^b \end{bmatrix} \\ &= \begin{bmatrix} \boldsymbol{S}(\boldsymbol{\omega}^b)\boldsymbol{I}^b\boldsymbol{\omega}^b + m^b\boldsymbol{S}(\boldsymbol{c}^b)\boldsymbol{S}(\boldsymbol{\omega}^b)\boldsymbol{v}^b \\ m^b\boldsymbol{S}(\boldsymbol{\omega}^b)\boldsymbol{S}(\boldsymbol{c}^b)^T\boldsymbol{\omega}^b + m^b\boldsymbol{S}(\boldsymbol{\omega}^b)^T\boldsymbol{v}^b \end{bmatrix}. \end{aligned} \tag{3}$$

The net force $\mathbf{f}^b$ in a robotic system is typically the combination of the actuators force $\mathbf{f}_a^b$, the viscous friction forces $\mathbf{f}_f^b = -\mathbf{b} \circ \mathbf{v}^b$, where $\circ$ is the Hadamard or entrywise product, and gravitational forces $\mathbf{f}_g^b$. Thus, if $\mathbf{f}^b = \mathbf{f}_a^b + \mathbf{f}_f^b + \mathbf{f}_g^b$, combining the equations (2) and (3) and replacing into (1), the Newton-Euler equations are:

$$\mathbf{f}_z^b = \begin{bmatrix} \boldsymbol{I}^b\dot{\boldsymbol{\omega}}^b + \boldsymbol{S}(\boldsymbol{\omega}^b)\boldsymbol{I}^b\boldsymbol{\omega}^b - \boldsymbol{S}(\ddot{\boldsymbol{d}}_0^b)m^b\boldsymbol{c}^b + \boldsymbol{b}_{\boldsymbol{\omega}} \circ \boldsymbol{\omega}^b \\ m^b\ddot{\boldsymbol{d}}_0^b + \boldsymbol{S}(\dot{\boldsymbol{\omega}}^b)m^b\boldsymbol{c}^b + \boldsymbol{S}(\boldsymbol{\omega}^b)\boldsymbol{S}(\boldsymbol{\omega}^b)m^b\boldsymbol{c}^b + \boldsymbol{b}_{\boldsymbol{v}} \circ \boldsymbol{v}^b \end{bmatrix}. \tag{4}$$

where $\mathbf{f}_z^b \stackrel{def}{=} \mathbf{f}_a^b + \mathbf{f}_g^b$ is the measured spatial force acting on the body including the actuators and gravitational forces, and $\boldsymbol{b}_{\boldsymbol{\omega}} = \mathbf{b}_{1:3}$, $\boldsymbol{b}_{\boldsymbol{v}} = \mathbf{b}_{4:6}$ are the vectors of rotational and translational viscous friction coefficients.

Since the mass m^b can be is estimated from the term $m^b\ddot{\boldsymbol{d}}_0^b$ in (4) separately from the terms containing $m^b\boldsymbol{c}^b$, it is possible to extract also the center of mass $\boldsymbol{c}^b$. To this end, the inertia matrix is written in vector for as $\bar{\boldsymbol{I}}^b = [I_{11}\ I_{12}\ I_{13}\ I_{22}\ I_{23}\ I_{33}]^T$, and the terms in (4) rearranged in such a way so that (4) can be written as linear expression with respect to the parameters:

$$\mathbf{f}_z^b = \begin{bmatrix} \mathbf{0}_{3\times1} & -\boldsymbol{S}(\ddot{\boldsymbol{d}}_0^b) & \boldsymbol{L}(\dot{\boldsymbol{\omega}}^b) + \boldsymbol{S}(\boldsymbol{\omega}^b)\boldsymbol{L}(\boldsymbol{\omega}^b) & \boldsymbol{D}(\boldsymbol{\omega}^b) & \mathbf{0}_{3\times3} \\ \ddot{\boldsymbol{d}}_0^b & \boldsymbol{S}(\dot{\boldsymbol{\omega}}^b) + \boldsymbol{S}(\boldsymbol{\omega}^b)\boldsymbol{S}(\boldsymbol{\omega}^b) & \mathbf{0}_{3\times6} & \mathbf{0}_{3\times3} & \boldsymbol{D}(\boldsymbol{v}^b) \end{bmatrix} \begin{bmatrix} m^b \\ m^b\boldsymbol{c}^b \\ \bar{\boldsymbol{I}}^b \\ \boldsymbol{b}_{\boldsymbol{\omega}} \\ \boldsymbol{b}_{\boldsymbol{v}} \end{bmatrix}$$
$$= \boldsymbol{A}^b\boldsymbol{\phi}^b. \tag{5}$$

where $\boldsymbol{L} : \mathbb{R}^3 \rightarrow \mathbb{R}^{3\times6}$ is a left-multiplication operator defined such that $\boldsymbol{L}(\boldsymbol{v})\bar{\boldsymbol{I}}^b = \boldsymbol{I}^b\boldsymbol{v}$, $\boldsymbol{D}(\boldsymbol{v}) = \text{diag}(\boldsymbol{v})$, $\boldsymbol{A}^b \in \mathbb{R}^{6\times16}$ is a matrix of containing the body's velocity and acceleration measurements, and $\boldsymbol{\phi}^b \in \mathbb{R}^{16}$ is the vector of the 10 unknown inertial parameters and 6 friction parameters. From (5), the ordinary least-squares (OLS) estimator is built as

$$\hat{\boldsymbol{\phi}}^b = \left(\boldsymbol{A}^{bT}\boldsymbol{A}^b\right)^{-1}\boldsymbol{A}^{bT}\mathbf{f}_z^b \tag{6}$$

The estimation of the inertial parameters $\boldsymbol{\phi}^b$ can also be formulated in a recursive way using, for example, a recursive least-squares (RLS) filter (Haykin, 2013), or other recursive strategies using total least-squares as proposed in (Kubus et al., 2008) for the estimation of loads attached to fixed-base robot manipulators. Unlike traditional least-squares, total least-squares approaches and recent improvements, such as the recursive restricted total least-squares (RTL) (Rhode et al., 2014) can handle noise on the outputs and the inputs, and not only the outputs.

3. PROPOSED APPROACH

The proposed strategy can be summarized in the following steps:

Step 1 : *Trajectory design that guarantees identifiability of the parameters.*

Step 2 : *Compute the mutual information content* $\hat{I}(\bar{\mathbf{a}}_k^b; \bar{\mathbf{f}}_k^b)$ *between sequences of data of applied spatial forces:*

$$\bar{\mathbf{f}}_k^b \overset{def}{=} \{\mathbf{f}_i^b; k-N \leq i \leq k\}$$

and the measured spatial accelerations:

$$\bar{\mathbf{a}}_k^b \overset{def}{=} \{\mathbf{a}_i^b; k-N \leq i \leq k\}.$$

Step 3 *:* Solve the recursive least-squares (RLS) estimation with the data sequences $\{\bar{\boldsymbol{A}}_k^b; \bar{\mathbf{f}}_k^b\}$, for which $\hat{I}(\bar{\mathbf{a}}_k^b; \bar{\mathbf{f}}_k^b) > 0$, *where* $\bar{\boldsymbol{A}}_k^b$ *is the data matrix constructed by vertically stacking matrices* $\boldsymbol{A}^b(\mathbf{a}_i^b, \mathbf{v}_i^b)$*, from (5) for* $k-N \leq i \leq k$*, i.e.*

$$\bar{\boldsymbol{A}}_k^b \overset{def}{=} [\boldsymbol{A}^b(\mathbf{a}_{k-N}^b, \mathbf{v}_{k-N}^b)^T,\ \boldsymbol{A}^b(\mathbf{a}_{k-N+1}^b, \mathbf{v}_{k-N+1}^b)^T,\ \boldsymbol{A}^b(\mathbf{a}_{k-N+2}^b, \mathbf{v}_{k-N+2}^b)^T,\ \ldots,\ \boldsymbol{A}^b(\mathbf{a}_k^b, \mathbf{v}_k^b)^T]^T.$$

The details of each step are discussed in the following subsections.

3.1 Trajectories for identifiability

The motions that excite a robot's dynamics and ensure the identifiability of the inertial parameters are called persistent exciting (PE) trajectories or optimal excitation trajectories (Gautier and Khalil, 1992; Park, 2006). The PE trajectories are typically sinusoidal and polynomial functions that minimize the sensitivity of the estimated parameters to measurement noise and disturbances. The trajectories must be designed to ensure that $\boldsymbol{A}^{bT}\boldsymbol{A}^b$ in (5) is invertible. It can easily be verified that $\boldsymbol{A}^{bT}\boldsymbol{A}^b$ becomes not invertible due to loss of rank when either the trajectory is purely translational, i.e. $(\dot{\boldsymbol{\omega}}^b, \boldsymbol{\omega}^b) = (\mathbf{0}, \mathbf{0})$, or purely rotational, i.e. $(\dot{\boldsymbol{v}}^v, \boldsymbol{v}^b) = (\mathbf{0}, \mathbf{0})$. However, the loss of rank does not affect the possibility of identifying the remaining parameters. Thus, it is convenient to group the identifiable parameters into rotational and translational parameters, and implement the identification process in two separate stages.

Stage 1 : For a straight trajectory with $(\dot{\boldsymbol{\omega}}^b, \boldsymbol{\omega}^b) = (\mathbf{0}, \mathbf{0})$, set all components of $\mathbf{f}^b$ to zero, except for the longitudinal motion force $f_x = \frac{A}{T}\left|(t \text{mod} T) - \frac{T}{2}\right| + f_0$ and solve the following reduced version of (5):

$$\begin{bmatrix} \ddot{\boldsymbol{d}}_0^b & \boldsymbol{D}(\boldsymbol{v}^b) \end{bmatrix} \begin{bmatrix} m^b \\ \boldsymbol{b}_{\boldsymbol{v}} \end{bmatrix} = \begin{bmatrix} f_x \\ 0 \\ 0 \end{bmatrix}. \tag{7}$$

Stage 2 : For a purely rotational maneuver with $(\dot{\boldsymbol{v}}^b, \boldsymbol{v}^b) = (\mathbf{0}, \mathbf{0})$, set all components of $\mathbf{f}^b$ to zero, except for the rotational torque $\tau_z = \frac{A}{T}\left|(t \text{mod} T) - \frac{T}{2}\right| + \tau_0$ and solve the following reduced version of (5):

$$\begin{bmatrix} \boldsymbol{L}(\dot{\boldsymbol{\omega}}^b) + \boldsymbol{S}(\boldsymbol{\omega}^b)\boldsymbol{L}(\boldsymbol{\omega}^b) & \boldsymbol{D}(\boldsymbol{\omega}^b) \end{bmatrix} \begin{bmatrix} \bar{\boldsymbol{I}}^b \\ \boldsymbol{b}_{\boldsymbol{\omega}} \end{bmatrix} = \begin{bmatrix} 0 \\ 0 \\ \tau_z \end{bmatrix}. \tag{8}$$

Stage 3 : For an arc traversed at constant longitudinal and angular velocities with $(\dot{\boldsymbol{v}}^b, \boldsymbol{v}^b) = (\mathbf{0}, \boldsymbol{v}_e^b)$, $(\dot{\boldsymbol{\omega}}^b, \boldsymbol{\omega}^b) = (\mathbf{0}, \boldsymbol{\omega}_e^b)$, and a constant spatial force $\mathbf{f}^b = [0\ 0\ \tau_{z_e}\ f_{x_e}\ 0\ 0]^T$ solve the following reduced version of (5):

$$\boldsymbol{S}(\boldsymbol{\omega}^b)\boldsymbol{S}(\boldsymbol{\omega}^b)\boldsymbol{c}^b = \frac{f_x}{\hat{m}^b} - \frac{\hat{b}_{v_x}}{\hat{m}^b}v_x^b. \tag{9}$$

This strategy helps to decouple the estimation of one set of parameters from disturbances and noise induced by the other control action associated to the other parameters and viceversa.

3.2 Mutual information content criterion

The mutual information content $I(\bar{\mathbf{a}}_k^b; \bar{\mathbf{f}}_k^b)$ criterion is employed to select measurements that contribute to the improvement of the estimates and discard measurement sequences that have a poor signal-to-noise ratio or have a weak dependence. In other words, without a sufficiently large change in the forces $\bar{\mathbf{f}}_k^b$ driving the system, the accelerations will be null or practically negligible, therefore it becomes hard to find any evidence about how the input forces affect the accelerations, and in turn the velocities, which will be almost constant because the accelerations will be negligible. Thus the quality of data for identifiability of the parameters can be assessed using a mutual dependence criterion, such as the mutual information measure (Smith, 2015). In terms of the probability density functions for continuous distributions $\bar{\mathbf{a}}_k^b$ and $\bar{\mathbf{f}}_k^b$, the mutual information measure is defined as:

$$I(\bar{\mathbf{a}}_k^b; \bar{\mathbf{f}}_k^b) = \int_{\bar{\mathbf{a}}_k^b}\int_{\bar{\mathbf{f}}_k^b} p(\bar{\mathbf{a}}_k^b; \bar{\mathbf{f}}_k^b) \log\left(\frac{p(\bar{\mathbf{a}}_k^b; \bar{\mathbf{f}}_k^b)}{p(\bar{\mathbf{a}}_k^b)p(\bar{\mathbf{f}}_k^b)}\right) \partial\bar{\mathbf{a}}_k^b \partial\bar{\mathbf{f}}_k^b.$$

The marginal probability density functions $p(\bar{\mathbf{a}}_k^b)$, $p(\bar{\mathbf{f}}_k^b)$ and the joint probability density function $p(\bar{\mathbf{a}}_k^b; \bar{\mathbf{f}}_k^b)$ are

not known, but by an adequate the design of the exciting trajectory driving forces can be made to approach normal distributions, in which case the mutual information criterion can be expressed in terms of the correlation $\rho(\bar{\mathbf{a}}_k^b; \bar{\mathbf{f}}_k^b)$ as (Gel'fand and Yaglom, 1957):

$$I(\bar{\mathbf{a}}_k^b; \bar{\mathbf{f}}_k^b) = -\frac{1}{2} \log \left(1 - \rho(\bar{\mathbf{a}}_k^b; \bar{\mathbf{f}}_k^b)^2\right). \tag{10}$$

It is to be noted that the mutual information criterion is positive also for negative correlations $\rho(\bar{\mathbf{a}}_k^b; \bar{\mathbf{f}}_k^b) < 0$ and that $I(\bar{\mathbf{a}}_k^b; \bar{\mathbf{f}}_k^b) \to 0$ when $\rho(\bar{\mathbf{a}}_k^b; \bar{\mathbf{f}}_k^b)^2 \to 0$. However, from the equations of motion (7) or (8) it is possible to observe that for a given velocity possibly non-zero, the elements of the spatial acceleration $\mathbf{a}^b$ will be positive for a positive spatial force $\mathbf{f}^b$ acting along the axes of the spatial acceleration that are also positive if the spatial force $\mathbf{f}^b$ exceeds the viscous force. Hence, negative correlations between the measured acceleration and an applied excitation can only occur when the applied excitation is not able to produce a force that overcomes the effects of friction. Thus, in order to obtain better estimates of the inertial parameters, we propose a variant of the mutual information criterion (10), which we define here as:

$$\hat{I}(\bar{\mathbf{a}}_k^b; \bar{\mathbf{f}}_k^b) = -\frac{1}{2} \log \left(1 - \rho(\bar{\mathbf{a}}_k^b; \bar{\mathbf{f}}_k^b)\right). \tag{11}$$

The *mutual information content* index (11) employs $\rho(\bar{\mathbf{a}}_k^b; \bar{\mathbf{f}}_k^b)$ instead of $\rho(\bar{\mathbf{a}}_k^b; \bar{\mathbf{f}}_k^b)^2$, therefore when $\rho(\bar{\mathbf{a}}_k^b; \bar{\mathbf{f}}_k^b) < 0$, then $\hat{I}(\bar{\mathbf{a}}_k^b; \bar{\mathbf{f}}_k^b) < 0$. This allows to select measurement sequences which are consistent with the expected dependence between the variables imposed by the physical laws. *Remark: Under the assumption of normal distributions, using the correlation coefficient $\rho(\bar{\mathbf{a}}_k^b; \bar{\mathbf{f}}_k^b)$ directly as measure of dependence is equivalent. However, it is well-known that, while independent variables have a correlation coefficient $\rho = 0$, uncorrelated signals with $\rho = 0$ are not necessarily independent. Ongoing work concerns developing strategies to obtain estimates of the marginal and joint distributions of the data in order to improve the information content estimate without the assumptions that have been considered in this work to render the approach feasible for practical implementation of a real-time online inertial parameter estimator.*

3.3 Recursive least-squares estimation

The recursive least-squares estimator (Söderström and Stoica, 1989) is implemented to recursively update the parameters estimate in each of the three estimation problems of stage 1, 2 and 3. For simplicity of exposition, consider a general data matrix $\bar{\boldsymbol{A}}_k^b$ containing a sequence of values of the measured acceleration and velocities $\bar{\mathbf{a}}_k^b$ and $\bar{\mathbf{v}}_k^b$, and consider a vector with measurements of the applied excitation force $\bar{\mathbf{f}}_k^b$, and let $\hat{\boldsymbol{\phi}}_0^b$ be the initial estimate obtained from the solution of the ordinary least squares (OLS) problem (6). The recursive least-squares (RLS) estimator of the parameters $\hat{\boldsymbol{\phi}}_k^b$ at instant k is computed by adjusting the previous $\hat{\boldsymbol{\phi}}_{k-1}^b$ according to the magnitude of the residuals (estimation error $\boldsymbol{e}_k$) and the following steps:

$$\boldsymbol{e}_k = \bar{\mathbf{f}}_k^b - \bar{\boldsymbol{A}}_k^b \hat{\boldsymbol{\phi}}_{k-1}^b \tag{12}$$

$$\boldsymbol{K}_k = \boldsymbol{P}_k \bar{\boldsymbol{A}}_k^b = \boldsymbol{P}_{k-1} \bar{\boldsymbol{A}}_k^b \left[\lambda \boldsymbol{I} + \bar{\boldsymbol{A}}_k^{b\,T} \boldsymbol{P}_{k-1} \bar{\boldsymbol{A}}_k^b\right]^{-1} \tag{13}$$

$$\boldsymbol{P}_k = \lambda^{-1} \boldsymbol{P}_{k-1} - \lambda^{-1} \boldsymbol{K}_k \bar{\boldsymbol{A}}_k^{b\,T} \boldsymbol{P}_{k-1} \tag{14}$$

$$\hat{\boldsymbol{\phi}}_k^b = \hat{\boldsymbol{\phi}}_{k-1}^b + \boldsymbol{K}_k \boldsymbol{e}_k \tag{15}$$

The standard initialization of estimator covariance matrix $\lambda^2 \boldsymbol{P}_0$ is to set $\boldsymbol{P}_0 = \frac{1}{\sigma^2} \boldsymbol{I}$, where σ^2 is the minimum variance of the measurements data matrix $\bar{\boldsymbol{A}}^b$ (Söderström and Stoica, 1989). The *forgetting factor* λ is typically set to values slightly smaller than 1. The smaller the value, the quicker the past information will be forgotten.

3.4 Other estimation approaches

Two other parameter estimation approaches in addition to OLS and RLS have been implemented for benchmarking purposes. One is the *Feasible Generalized Least Squares* (FGLS), which is an implementable practical generalization of the weighted-least squares approach. The FGLS estimator is similar to the OLS estimator of equation (6), but includes the inverse of the covariance matrix of the residuals $\boldsymbol{\Omega}$, (Baltagi, 2008):

$$\hat{\boldsymbol{\phi}}^b = \left(\boldsymbol{A}^{b\,T} \boldsymbol{\Omega}^{-1} \boldsymbol{A}^b\right)^{-1} \boldsymbol{A}^{b\,T} \boldsymbol{\Omega}^{-1} \mathbf{f}_z^b \tag{16}$$

For computational simplicity, the covariance matrix of the residuals $\boldsymbol{\Omega}$ is defined as $\boldsymbol{\Omega} = \text{diag}(\sigma_1^2, \sigma_2^2, \ldots, \sigma_n^2)$ with $\sigma_i = r_i = \left[\bar{\mathbf{f}}_k^b - \bar{\boldsymbol{A}}_k^b \hat{\boldsymbol{\phi}}_{k-1}^b\right]_i$, where $[\boldsymbol{v}]_i$ represents the i-th element of vector $\boldsymbol{v}$.

The other approach considered for evaluation is the *Total Least Squares* method. This approach does not assume that $\boldsymbol{A}_k^b$ is noise-free like the OLS does. A recursive formulation can be found in (Kubus et al., 2008).

4. RESULTS AND DISCUSSION

4.1 Testing methodology

The proposed parameter estimation approach is evaluated in simulations and experimentally using an industrial compact skid-steer loader Cat®262C shown in Fig. 1 (a), which is equipped with two torque sensors by Manner Sensortelemetrie (see Fig. 1 (b)), one Sensonor IMU, two VectorNav IMUs, four SICK LMS511 lidars, one Piksi SwiftNav RTK-DGPS, TE Connectivity MEAS inclination sensors, wheel encoders, a control and navigation computer and wireless communication interfaces to make it semi-autonomous. The control computer runs ROS Melodic to acquire the sensors' measurements at a rate of 100 Hz.

The skid-steer loader has a right and a left hydraulic gear motor that drives a chain-pinion system for the right and left wheels, respectively. The torque sensors are located on the front wheels. The measured right and left wheel torques are τ_r and τ_l. These torques are employed to calculate the total longitudinal force f_x and turning torque τ_z, which are given by:

(a)

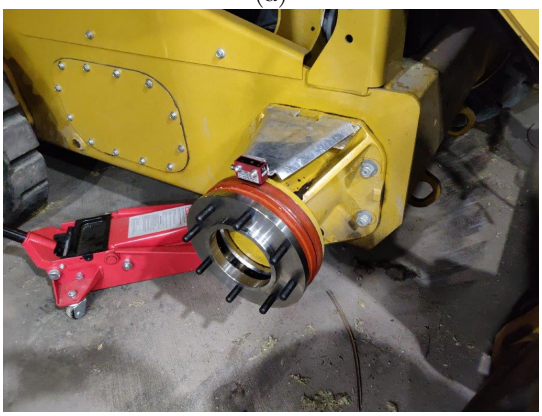

(b)

Fig. 1. Experimental setup with Cat®262C loader: (a) Robotic skid-steer loader, (b) Front-right wheel torque sensor.

$$f_x = \frac{\tau_r + \tau_l}{r_{\text{wheel}}} \tag{17}$$

$$\tau_z = \frac{\tau_r - \tau_l}{r_{\text{wheel}}} \frac{L_{\text{base}}}{2} \tag{18}$$

where r_{wheel} is the wheel radius and L_{base} is the length of the front and rear axles. Complete details about the dynamic model of the skid-steer loader employed can be found in Aguilera-Marinovic et al. (2017).

4.2 Simulation results

The proposed approach was first tested in simulations implemented in Python 3.6 using a physically accurate model of the skid-steer Cat 262 developed in (Aguilera-Marinovic et al., 2017). From the simulations it was possible to verify a suitable excitation signal and determine the minimum signal-to-noise ratio required for adequate estimation. Excitation torques in the form of a triangular signal were employed because this ensures $\mathbf{a}^b \neq 0$, thus preventing that $A_b^T A_b$ does not become non-invertible. The application of a triangular waveform produces a consistent acceleration response that reaches a peak value due to the viscous friction force, which limits the net acceleration amplitude, as shown in Fig. 2. If T is the response time of the machine to a step input, the simulation results confirm that an adequate excitation waveform should have a period $T_{\mathbf{f}} \approx 3T$ to allow for the response to stabilize. The length in time $T_{\hat{\phi}}$ of the estimation window should be selected such that $T \leq T_{\hat{\phi}} \leq T_{\mathbf{f}}$. The simulation shows that

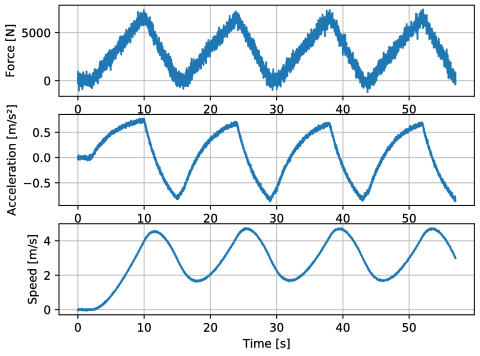

Fig. 2. Longitudinal applied force f_x, acceleration a_x and speed v_x for the simulated robotic skid-steer.

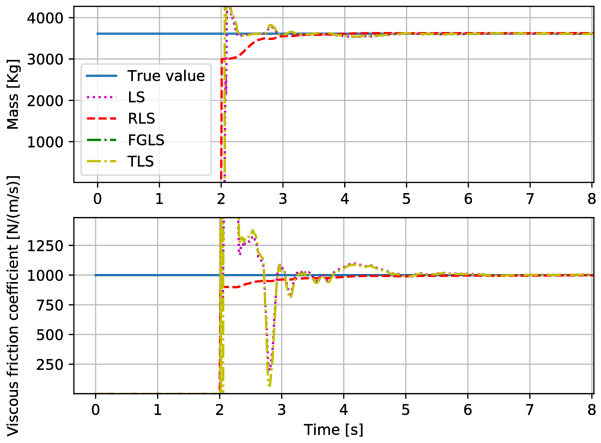

Fig. 3. Simulation results for a linear motion.

$T \approx 5$ s, therefore $T_{\mathbf{f}} = 15$ s. The mass estimation RMS errors for different lengths $T_{\hat{\phi}}$ of the estimation window are summarized in Table 1, which shows that $T_{\hat{\phi}} = 10$ s is an optimal window length that minimizes the estimation error for LS, RLS, FGLS and TLS.

The evolution in time of the estimated inertial parameters for each of the approaches was computed applying a purely longitudinal motion force and using the optimal window length $T_{\hat{\phi}} = 10$ s. The results in Fig. 3 show that the ordinary LS estimation approach has the fastest convergence to the model mass m and behaves very similar to FGLS and TLS. On the other hand, RLS is slower to converge, but less sensitive to noise. Similarly, applying forces that produce a purely rotational motion, the approaches yield the rotational inertia and viscous friction parameters as shown in Fig 4.

4.3 Experimental results

Analogous experiments to those performed in simulations were carried out with the real skid-steer loader. A measurement sequence of a longitudinal motion experiment is shown in Fig. 5, which illustrates a typical velocity and acceleration profile corresponding to a regular full throttle starting and stopping maneuver. It is possible to observe that the measured force is significantly noisier than in simulations. Hence, a moving mean filter of 10 samples

$T_{\hat{\phi}}$ [s]	2	3	4	5	6	7	8	9	10	15	20	25	30
LS	79.46	116.24	34.86	17.91	14.26	92.31	32.37	44.91	11.66	26.2	9.35	1.58	1.22
RLS	50.26	72.48	18.72	56.59	4.27	5.45	18.55	31.56	3.89	54.09	9.29	13.52	16.32
FGLS	79.99	115.61	34.79	18.47	14.04	93.79	32.17	45.25	11.62	26.03	9.34	1.63	1.45
TLS	189.95	310.4	84.82	68.74	92.11	187.35	12.24	64.72	3.25	48.42	12.38	23.42	23.65

Table 1. Estimation RMS error [kg] for each approach at different estimation window lengths $T_{\hat{\phi}}$.

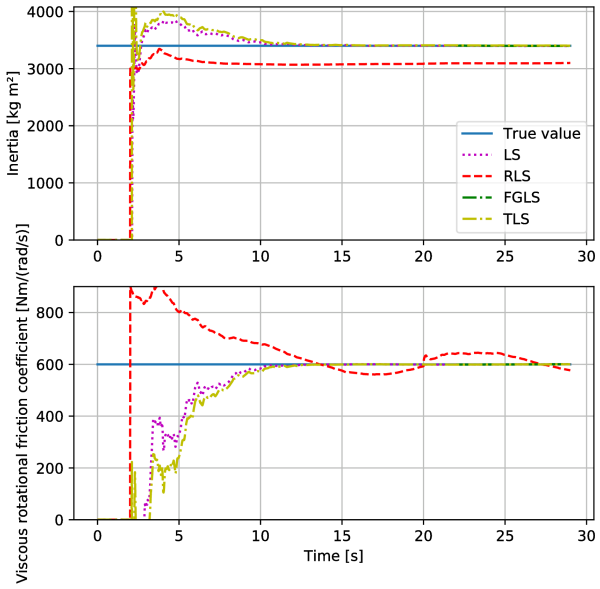

Fig. 4. Simulation results for a rotational motion.

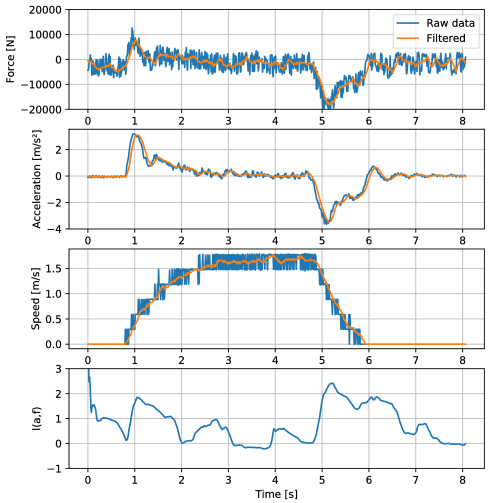

Fig. 5. Measured longitudinal force f_x, acceleration a_x, speed v_x and mutual information criterion $\hat{I}(\bar{\mathbf{a}}_k^b; \bar{\mathbf{f}}_k^b)$ for the robotic skid-steer loader.

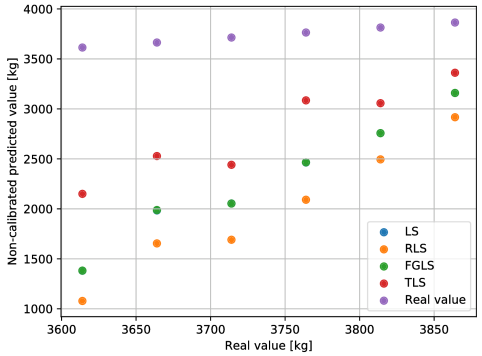

Fig. 6. Non-calibrated predicted mass versus real mass.

(0.1 s) was applied to the measurements. On the other hand, the response of the force to a change in the pulse-width modulated signal driving the hydraulic servo-valves does not follow the triangular waveform of the simulations. This is due to the servo-valve characteristics. Nonetheless, the real excitation produces a clear change in acceleration and a corresponding change in speed, which are adequate for estimating the inertial parameters. The mutual information criterion $\hat{I}(\bar{\mathbf{a}}_k^b; \bar{\mathbf{f}}_k^b)$ computed for the measured acceleration and forces is shown in the fourth plot of Fig. 5. It is possible to observe that information content is larger during the acceleration or deceleration period. However, the experiments show that the force during deceleration is different to the force during acceleration. This is due to the fact that the pump-motor and the motor-reservoir hydraulic circuits are different and the associated time constants are not the same. Moreover, the torque is located between the actuated axle and the wheel, but during braking is not the motor the one that is applying the braking force as when the motor is applying the acceleration force. In fact, the energy is dissipated in the return circuit of the hydraulic fluid. Therefore, for real applications only acceleration maneuvers can be used to adequately estimate the inertial parameters.

In order to validate the approach's capacity to estimate changes in the transported mass, as would occur in a real loading task, five water drums weighing 50 kg each were added gradually to the skid-steer loader whose mass is $m =$ 3614 kg when it is not loaded. The experiments to identify the inertial parameters were repeated 9 times with each weight using the data satisfying the mutual information criterion $\hat{I}(\bar{\mathbf{a}}_k^b; \bar{\mathbf{f}}_k^b) \geq 0.7$ and an estimation window $T_{\hat{\phi}} =$ 3.2 s (320 samples, sampled at $f_s = 100$ Hz). The predicted weight by LS, RLS, FGLS and TLS before calibration are shown in Fig. 6. It is possible to observe estimates that are consistent with a linearly increasing value. However, the estimates do not match the true values. Therefore, a calibration function is employed to adjust the estimates and take into account gains and offsets in the signal conditioning circuits employed to scale the torque sensor voltage outputs to the right levels for analog-to-digital conversion in the data-acquisition module.

	LS	RLS	FGLS	TLS
α	0.146	0.140	0.146	0.191
β	3401.4	3459.9	3401.1	3208.8

Table 2. Coefficients of the calibration function (19).

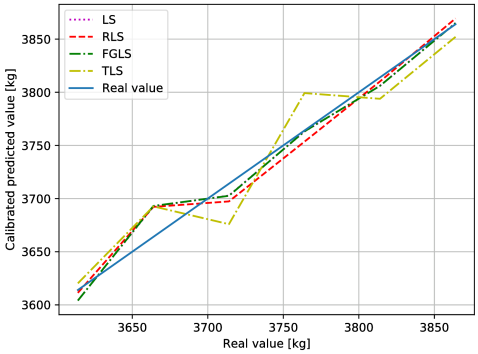

Fig. 7. Corrected mass prediction versus real mass.

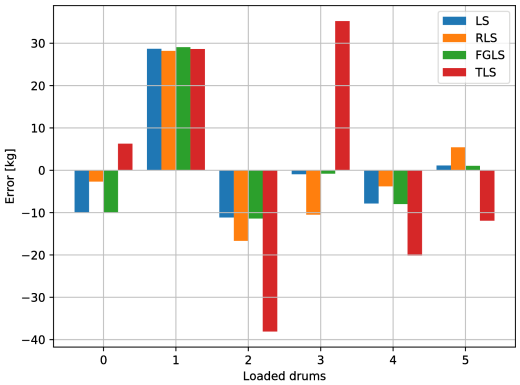

Fig. 8. Corrected prediction RMS errors for each load.

The calibration function for the mass estimate is defined as:

$$\hat{m}_c = \alpha\hat{m} + \beta, \tag{19}$$

where $\hat{m}$ is the original non-calibrated mass estimate and $\hat{m}_c$ is the calibrated estimate. The parameters α and β are found as the solution to a least-squares problem formulated to minimize the prediction error, i.e. $\alpha, \beta = \arg\min_{\alpha,\beta} \sum_{i=0}^{N} |m_i^* - \hat{m}_c(\hat{m}_i; \alpha, \beta)|^2$, where m_i^* is the i-th calibration mass in a set of $N = 5$ calibration masses. The coefficients α and β found are summarized in Table 2 and the predicted masses using the calibration function are shown in Fig. 7. The predicted mass RMS errors for each load and estimation approach are presented in the bar plot of Fig. 8.

The analysis of the practical threshold for the mutual information criterion and the estimation window size in number of samples is summarized in Tables 3 and 4, respectively. It is possible to observe from Table 3 that most of the methods yield the smallest mass estimation RMS error for a threshold of 0.7. Concerning the size of the estimation window, the smallest estimation RMS error for the mass is achieved with a 400 samples sliding window, which is equivalent to 4 s of acquired data.

$\hat{I}(\bar{\mathbf{a}}_k^b; \bar{\mathbf{f}}_k^b)$	LS	RLS	FGLS	TLS
0.5	22.6	36.4	22.6	25.6
0.7	5.1	42.6	4.9	21.3
0.9	4.9	10.4	4.9	21.3
1.1	20.4	11.1	20.4	31.7
1.3	15.2	9.8	21.8	19.9
1.5	30.7	10.7	26.2	30.6

Table 3. Mass estimation RMS error for different threshold values for the mutual information criterion.

N° samples	LS	RLS	FGLS	TLS
200	11.8	23.2	11.8	24.2
300	4.9	10.9	4.9	19.5
400	4.9	10.4	4.9	24.0
500	17.5	12.1	17.5	31.3
600	17.5	12.4	67.1	28.2
700	15.1	12.4	63.7	28.6

Table 4. Mass estimation RMS error for different threshold values for different estimation window sizes.

5. CONCLUSIONS

An approach for online inertial and friction parameters estimation of robotic loaders was presented. The approach combines the least squares estimation with an information content criterion and a suitable excitation. This methodology is tested both in simulation and experimentally using a semi-autonomous Cat®262C compact skid-steer loader equipped with inertial and torque sensors between the actuated axle and the wheels. The results show that the approach produces accurate estimates without degrading, unlike the standard recursive least squares approaches.

On average, the estimation error in simulation was 0.0008%±0.03% and 0.15%±0.13% in the experiments, with a 95% confidence level. These values are at least 80% smaller than those obtained using a traditional recursive least squares estimator without the information criterion. The use of the mutual information between the excitation force and the measured acceleration is crucial to handle low acceleration situations that render the estimation problem ill-posed and often occur at the beginning of motion or during constant velocity motion part of a trajectory.

Ongoing work concerns the validation of the proposed method using different trajectories, as indicated in Stages 2 and 3 of section 3.1, in addition to the purely linear motion experiments. Thus to show that also the rotational inertia and center of mass variations due to changes in the load can be estimated in practice and not only in simulation.

The proposed approach can be valuable for productivity monitoring and adaptive motion control of autonomous machines with variable loads, such as loaders, excavators and trucks in construction, forestry and mining. Accurate knowledge of the friction related parameters is also important, as this can provide the basis for further research into machine wear and predictive maintenance schemes.

ACKNOWLEDGEMENTS

This project has been supported by the National Commission for Science and Technology Research of Chile (Conicyt) under Fondecyt grant 1171760, Basal FB0008 and Fondequip grant 120141.

REFERENCES

Aguilera-Marinovic, S., Torres-Torriti, M., and Auat-Cheein, F. (2017). General dynamic model for skid-steer mobile manipulators with wheel-ground interactions. *IEEE/ASME Transactions on Mechatronics*, 22(1), 433–444. doi:10.1109/TMECH.2016.2601308.

Baltagi, B. (2008). *Econometric analysis of panel data*. John Wiley & Sons.

Featherstone, R. (2008). *Rigid Body Dynamics Algorithms*. Springer-Verlag New York, Inc., Secaucus, NJ, USA. doi:10.1007/978-1-4899-7560-7.

Franchi, A., Petitti, A., and Rizzo, A. (2014). Distributed estimation of the inertial parameters of an unknown load via multi-robot manipulation. In *53rd IEEE Conference on Decision and Control*. IEEE. doi:10.1109/cdc.2014.7040346.

Gautier, M. and Khalil, W. (1992). Exciting trajectories for the identification of base inertial parameters of robots. *The International Journal of Robotics Research*, 11(4), 362–375. doi:10.1177/027836499201100408.

Gel'fand, I. and Yaglom, A. (1957). Calculation of the amount of information about a random function contained in another such function. *American Mathematical Society Translations*, Series 2(12), 199–246. English translation of original in Uspekhi Matematicheskikh Nauk 12 (1): 3-52.

Haykin, S. (2013). *Adaptive Filter Theory*. Prentice-Hall, Inc., Upper Saddle River, NJ, USA, 5 ed. edition.

Hoang, N.B. and Kang, H.J. (2015). Observer-based dynamic parameter identification for wheeled mobile robots. *International Journal of Precision Engineering and Manufacturing*, 16(6), 1085–1093. doi:10.1007/s12541-015-0140-z.

Kubus, D., Kroger, T., and Wahl, F. (2008). On-line estimation of inertial parameters using a recursive total least-squares approach. In *Intelligent Robots and Systems, 2008. IROS 2008. IEEE/RSJ International Conference on*, 3845–3852. doi:10.1109/IROS.2008.4650672.

Park, K.J. (2006). Fourier-based optimal excitation trajectories for the dynamic identification of robots. *Robotica*, 24(5), 625–633. doi:10.1017/S0263574706002712.

Rhode, S., Usevich, K., Markovsky, I., and Gauterin, F. (2014). A recursive restricted total least-squares algorithm. *Signal Processing, IEEE Transactions on*, 62(21), 5652–5662. doi:10.1109/TSP.2014.2350959.

Rigotti-Thompson, M., Torres-Torriti, M., Cheein, F.A., and Troni, G. (2018). $\mathcal{H}_\infty$ controller design for a robotic research and educational mining loader. In *2018 19th International Conference on Research and Education in Mechatronics (REM)*, 18–23. doi:10.1109/REM.2018.8421769.

Rogers-Marcovitz, F. and Kelly, A. (2014). On-line mobile robot model identification using integrated perturbative dynamics. In *Experimental Robotics*, 417–431. Springer Berlin Heidelberg. doi:10.1007/978-3-642-28572-1_29.

Seegmiller, N., Rogers-Marcovitz, F., Miller, G., and Kelly, A. (2013). Vehicle model identification by integrated prediction error minimization. *I. J. Robotics Res.*, 32(8), 912–931. doi:10.1177/0278364913488635.

Siciliano, B. and Khatib, O. (eds.) (2008). *Springer Handbook of Robotics*. Springer-Verlag Berlin Heidelberg. doi:10.1007/978-3-540-30301-5.

Smith, R. (2015). A mutual information approach to calculating nonlinearity. *Stat*, 4(1), 291–303. doi:10.1002/sta4.96.

Söderström, T. and Stoica, P. (eds.) (1989). *System Identification*. Prentice-Hall, Inc., Upper Saddle River, NJ, USA.